Traffic models of periodic event-triggered control systems

Fu, Anqi; Mazo, Manuel

DOI
10.1109/TAC.2018.2879763

Publication date
2019

Document Version
Final published version

Published in
IEEE Transactions on Automatic Control

Traffic Models of Periodic Event-Triggered Control Systems

Anqi Fu, *Student Member, IEEE*, and Manuel Mazo Jr., *Senior Member, IEEE*

***Abstract*—Periodic event-triggered control (PETC) [13] is a version of event-triggered control that only requires the measurement of the plant output periodically instead of continuously. In this note, we present a construction of timing models for these PETC implementations to capture the dynamics of the traffic they generate. In the construction, we employ a two-step approach. We first partition the state space into a finite number of regions. Then, in each region, the event-triggering behavior is analyzed with the help of linear matrix inequalities. The state transitions among different regions result from computing the reachable state set starting from each region within the computed event time intervals.**

***Index Terms*—Formal methods, linear matrix inequality (LMI), periodic event-triggered control (PETC), reachability analysis, systems abstractions.**

I. Introduction

Wireless networked control systems (WNCSs) are control systems that employ wireless networks as feedback channels. In such systems, the physically distributed components are co-located with their own wireless nodes and communicate via a wireless network. These components can be established, updated easily, and designed with great mobility once the nodes are supported by batteries. Because of this great adaptability of WNCSs, they have been attracting much attention. This adaptability, however, opens two major issues that must be considered while designing such systems: Limited bandwidth and energy supply.

Most often, control tasks are designed to be executed periodically. This periodic strategy, also named time-triggered control, does not regard the system's current state and, thus, may waste bandwidth and energy. Alternatively, event-triggered control (ETC) strategies are proposed to reduce bandwidth occupation; see, e.g., [5], [18], [20], [23], [26], [27], and references therein. In the ETC, the control tasks only execute when necessary, e.g., when some predesigned performance indicators are about to be violated. Thus, the systems are tightfisted in communication. However, to validate the predesigned event-triggering conditions, sensors are required to sample the plant output continuously. This continuous monitoring can consume large amounts of energy. To reduce this energy consumption, naturally, one may want to replace the continuous sampling by a discrete time sampling.

When applying discrete time sampling, to compensate the delay caused by the discretization, one can either design a stricter event-triggering condition based on the system dynamics, as in [19], or modify the Lyapunov function, as in [13]. In [13], Heemels *et al.* present a periodic event-triggered control (PETC) mechanism. In a PETC implementation, the sensors are only required to measure the plant output and validate the event conditions periodically. Only when some predesigned conditions are satisfied, fresh measurements are employed to recompute the controller output. Therefore, the PETC enjoys the benefits of both cautious communication and discrete time measurement. Compared with the work presented in [19], the event conditions can be less conservative to further reduce communications, thus reducing energy and bandwidth consumption as well. Furthermore, the transmissions of control inputs from the controller to the plant are also included in the PETC mechanism.

Taking full advantage of the scarce communications of ETC controllers is hindered by the inherent difficulty of scheduling such communications, be it to reuse the bandwidth or to save energy on listening times. To further reduce the resource consumption and to fully extract the potential gains from the ETC, the problem of scheduling ETC communications needs to be addressed. To enable such scheduling, a model of the traffic (to be scheduled) generated by the ETC is required. This is addressed in [16], wherein Kolarijani and Mazo propose approximate power quotient systems as finite models to capture the timing behaviors of ETC systems, applying the triggering mechanism from [23]. They first partition the state space into finite cones. In each cone, they analyze the timing behavior by overapproximation methods [3], [4], [6], [11], [14], [21], [22], linear matrix inequality (LMI) methods, and reachability analysis [2].

Similarly, in order to fully extract the potential gains from the PETC with scheduling approaches, a model for the traffic generated by the PETC is necessary. In this note, we extend the work presented in [16] to construct timing models of the PETC implementations from [13]. It is worth clarifying that our proposal, as in [16], does not affect the controller implementation, which remains (almost) identical to the one presented in [13]. We merely focus on providing models of traffic, i.e., abstractions of the whole PETC systems at the level required to design schedulers. As presented in [17], the constructed traffic models in this note are semantically equivalent to timed automata. Scheduling approaches for timed automata can be found in existing tools such as UPPAAL-Tiga [1].

In [16], state feedback controllers applying continuous output-measuring ETC are considered. In this note, we extend those results to output feedback systems applying discrete time (periodic) output feedback ETC. Taking as a starting point the work presented in [13] on PETC simplifies some of the constructions by reducing a line search over the reals (continuous time), as in [16], to a simple search over a countable set (the sampling instants) and by reducing the computation of a reachable set on a time interval to the reachable set at discrete time instants. Furthermore, the setting presented in [13] allows us to also

Manuscript received May 18, 2018; revised September 19, 2018; accepted October 25, 2018. Date of publication November 7, 2018; date of current version July 26, 2019. This work was supported in part by the European Research Council (ERC) Starting Grant SENTIENT 755953 and in part by China Scholarship Council (CSC) under Grant 201306020047. Recommended by Associate Editor L. Palopoli. *(Corresponding author: Anqi Fu.)*

A. Fu was with the Delft Center for Systems and Control, Delft University of Technology, Delft 2628CD, The Netherlands. He is now with the Department of Computing, Imperial College London, London SW72AZ, U.K. (e-mail: a.fu@imperial.ac.uk).

M. Mazo Jr. is with the Delft Center for Systems and Control, Delft University of Technology, Delft 2628CD, The Netherlands (e-mail: M.Mazo@tudelft.nl).

Color versions of one or more of the figures in this paper are available online at http://ieeexplore.ieee.org.

Digital Object Identifier 10.1109/TAC.2018.2879763

account for the presence of disturbances. Considering disturbances, however, makes the construction of the traffic models somewhat more complex, requiring a different type of partitioning than that presented in [16]. Finally, we remark that as opposed to the assumptions in [9], we do not require that the disturbance should vanish as the state converges. Instead, we only assume the disturbance to be both $\mathcal{L}_2$ and $\mathcal{L}_\infty$.

II. Notation and Preliminaries

We denote the n-dimensional Euclidean space by $\mathbb{R}^n$, the positive real numbers by $\mathbb{R}^+$, and $\mathbb{R}_0^+ = \mathbb{R}^+ \cup \{0\}$. The natural numbers, including zero, is denoted by $\mathbb{N}$. When zero is not included, we denote the natural numbers as $\mathbb{N}^+$. $\mathbb{IN}^+$ is the set of all closed intervals $[a, b]$ such that $a, b \in \mathbb{N}^+$ and $a \leq b$. For any set S, 2^S denotes the set of all subsets of S, i.e., the power set of S. $\mathcal{M}_{m\times n}$ and $\mathcal{M}_n$ are the set of all $m \times n$ real-valued matrices and the set of all $n \times n$ real-valued symmetric matrices, respectively. When $Q \subseteq Z \times Z$ is an equivalence relation on a set Z, $[z]$ denotes the equivalence class of $z \in Z$ and Z/Q denotes the set of all equivalence classes. By $|A|$, we denote the induced norm of a matrix. We define the space of all locally integrable signals with a finite $\mathcal{L}_2$-norm as $\mathcal{L}_2$ and the space of all signals with a finite $\mathcal{L}_\infty$-norm as $\mathcal{L}_\infty$. Now, we review some notions from the field of system theory.

Definition 2.1. (Metric) [7]: Consider a set T; $d : T \times T \to \mathbb{R} \cup \{+\infty\}$ is a metric (or a distance function) if the following three conditions are satisfied $\forall x,\ y,\ z \in T$: $d(x, y) = d(y, x)$, $d(x, y) = 0 \leftrightarrow x = y$, and $d(x, y) \leq d(x, z) + d(y, z)$. The ordered pair (T, d) is said to be a metric space.

Definition 2.2. (Hausdorff distance) [7]: Assume that X and Y are two nonempty subsets of a metric space (T, d). The Hausdorff distance $d_H(X, Y)$ is given by

$$\max\left\{\sup_{x\in X}\inf_{y\in Y} d(x, y), \sup_{y\in Y}\inf_{x\in X} d(x, y)\right\}. \tag{1}$$

Definition 2.3. (System) [24]: A system is a sextuple $(X, X_0, U, \longrightarrow, Y, H)$ consisting of the following:

1) a set of states X;
2) a set of initial states $X_0 \subseteq X$;
3) a set of inputs U;
4) a transition relation $\longrightarrow \subseteq X \times U \times X$;
5) a set of outputs Y;
6) an output map $H : X \to Y$.

The term finite-state (infinite-state) system indicates that X is a finite (an infinite) set. For a system, if the cardinality of U is smaller than or equal to one, then this system is said to be autonomous.

Definition 2.4. (Metric system) [24]: A system $\mathcal{S}$ is said to be a metric system if the set of outputs Y is equipped with a metric $d : Y \times Y \to \mathbb{R}_0^+$.

Definition 2.5. (Approximate simulation relation) [24]: Consider two metric systems $\mathcal{S}_a$ and $\mathcal{S}_b$ with $Y_a = Y_b$, and let $\epsilon \in \mathbb{R}_0^+$. A relation $R \subseteq X_a \times X_b$ is an ϵ-approximate simulation relation from $\mathcal{S}_a$ to $\mathcal{S}_b$ if the following three conditions are satisfied:

1) $\forall x_{a0} \in X_{a0}, \exists x_{b0} \in X_{b0}$ such that $(x_{a0}, x_{b0}) \in R$;
2) $\forall (x_a, x_b) \in R$, we have $d(H_a(x_a), H_b(x_b)) \leq \epsilon$;
3) $\forall (x_a, x_b) \in R$ such that $(x_a, u_a, x_a') \in \underset{a}{\longrightarrow}$ in $\mathcal{S}_a$ implies $\exists (x_b, u_b, x_b') \in \underset{b}{\longrightarrow}$ in $\mathcal{S}_b$ satisfying $(x_a', x_b') \in R$.

We denote the existence of an ϵ-approximate simulation relation from $\mathcal{S}_a$ to $\mathcal{S}_b$ by $\mathcal{S}_a \preceq_{\mathcal{S}}^{\epsilon} \mathcal{S}_b$ and say that $\mathcal{S}_b$ ϵ-approximately simulates $\mathcal{S}_a$ or $\mathcal{S}_a$ is ϵ-approximately simulated by $\mathcal{S}_b$. Whenever $\epsilon = 0$, the inequality $d(H_a(x_a), H_b(x_b)) \leq \epsilon$ implies $H_a(x_a) = H_b(x_b)$, and the resulting relation is called an (exact) simulation relation. We introduce the notion of a power quotient system and the corresponding lemma for later analysis.

Definition 2.6. (Power quotient system) [16]: Let $\mathcal{S} = (X, X_0, U, \longrightarrow, Y, H)$ be a system and R be an equivalence relation on X. The power quotient of $\mathcal{S}$ by R, denoted by $\mathcal{S}_{/R}$, is the system $(X_{/R}, X_{/R,0}, U_{/R}, \underset{/R}{\longrightarrow}, Y_{/R}, H_{/R})$ consisting of the following:

1) $X_{/R} = X/R$;
2) $X_{/R,0} = \{x_{/R} \in X_{/R} | x_{/R} \cap X_0 \neq \emptyset\}$;
3) $U_{/R} = U$;
4) $(x_{/R}, u, x'_{/R}) \in \underset{/R}{\longrightarrow}$ if $\exists (x, u, x') \in \longrightarrow$ in $\mathcal{S}$ with $x \in x_{/R}$ and $x' \in x'_{/R}$;
5) $Y_{/R} \subset 2^Y$;
6) $H_{/R}(x_{/R}) = \bigcup_{x\in x_{/R}} H(x)$.

Lemma 2.7: [16, Lem. 1]: Let $\mathcal{S}$ be a metric system, R be an equivalence relation on X, and let the metric system $\mathcal{S}_{/R}$ be the power quotient system of $\mathcal{S}$ by R. For any

$$\epsilon \geq \max_{x \in x_{/R},\, x_{/R} \in X_{/R}} d(H(x), H_{/R}(x_{/R})) \tag{2}$$

with d being the Hausdorff distance over the set 2^Y, and $\mathcal{S}_{/R}$ ϵ-approximately simulates $\mathcal{S}$, i.e., $\mathcal{S} \preceq_{\mathcal{S}}^{\epsilon} \mathcal{S}_{/R}$.

The definition of Minkowski addition is introduced here for the computation of the reachable sets.

Definition 2.8. (Minkowski addition): The Minkowski addition of two sets of vectors $\mathcal{A}$ and $\mathcal{B}$ in Euclidean space is performed by adding each vector in $\mathcal{A}$ to each vector in $\mathcal{B}$ as follows:

$$\mathcal{A} \oplus \mathcal{B} = \{\mathbf{a} + \mathbf{b} | \mathbf{a} \in \mathcal{A}, \mathbf{b} \in \mathcal{B}\}$$

where $\oplus$ denotes the Minkowski addition.

III. Problem Definition

The centralized PETC presented in [13] is reviewed here. Consider a continuous linear time-invariant plant of the following form:

$$\begin{cases} \dot{\xi}_p(t) = A_p \xi_p(t) + B_p \hat{v}(t) + E w(t) \\ y(t) = C_p \xi_p(t) \end{cases} \tag{3}$$

where $\xi_p(t) \in \mathbb{R}^{n_p}$ denotes the state vector of the plant, $y(t) \in \mathbb{R}^{n_y}$ denotes the plant output vector, $\hat{v}(t) \in \mathbb{R}^{n_v}$ denotes the input applied to the plant, and $w(t) \in \mathbb{R}^{n_w}$ denotes the perturbation. The plant is controlled by a discrete-time controller, given by

$$\begin{cases} \xi_c(t_{k+1}) = A_c \xi_c(t_k) + B_c \hat{y}(t_k) \\ v(t_k) = C_c \xi_c(t_k) + D_c \hat{y}(t_k) \end{cases} \tag{4}$$

where $\xi_c(t_k) \in \mathbb{R}^{n_c}$ denotes the state vector of the controller, $v(t_k) \in \mathbb{R}^{n_v}$ denotes the controller output vector, and $\hat{y}(t_k) \in \mathbb{R}^{n_y}$ denotes the input applied to the controller. A periodic sampling sequence is given by

$$\mathcal{T}_s := \{t_k | t_k := kh, k \in \mathbb{N}\} \tag{5}$$

where $h > 0$ is the sampling interval. Define two vectors as follows:

$$\begin{aligned} u(t) :&= \begin{bmatrix} y^{\mathrm{T}}(t) & v^{\mathrm{T}}(t) \end{bmatrix}^{\mathrm{T}} \in \mathbb{R}^{n_u} \\ \hat{u}(t_k) :&= \begin{bmatrix} \hat{y}^{\mathrm{T}}(t_k) & \hat{v}^{\mathrm{T}}(t_k) \end{bmatrix}^{\mathrm{T}} \in \mathbb{R}^{n_u} \end{aligned} \tag{6}$$

with $n_u := n_y + n_v$. $u(t)$ is the output of the implementation, and $\hat{u}(t)$ is the input of the implementation. A zero-order hold mechanism is applied between samplings to the input. At each sampling time t_k,

the input applied to the implementation $\hat{u}(t_k)$ is updated $\forall t_k \in \mathcal{T}_s$. Thus, we have

$$\hat{u}(t_k) = \begin{cases} u(t_k), & \text{if } \|u(t_k) - \hat{u}(t_k)\| > \sigma\|u(t_k)\| \\ \hat{u}(t_{k-1}), & \text{if } \|u(t_k) - \hat{u}(t_k)\| \leq \sigma\|u(t_k)\| \end{cases} \tag{7}$$

where $\sigma > 0$ is a given constant. Reformulating the event condition as a quadratic form, the event sequence can be defined as follows:

$$\mathcal{T}_e := \{t_b | b \in \mathbb{N}, t_b \in \mathcal{T}_s, \xi^{\mathrm{T}}(t_b) Q \xi(t_b) > 0\} \tag{8}$$

where $\xi(t) := \begin{bmatrix} \xi_p^{\mathrm{T}}(t) & \xi_c^{\mathrm{T}}(t) & \hat{y}^{\mathrm{T}}(t) & \hat{v}^{\mathrm{T}}(t) \end{bmatrix}^{\mathrm{T}} \in \mathbb{R}^{n_\xi}$, with $n_\xi := n_p + n_c + n_y + n_v$, and

$$Q = \begin{bmatrix} Q_1 & Q_2 \\ Q_2^{\mathrm{T}} & Q_4 \end{bmatrix}, \begin{cases} Q_1 = \begin{bmatrix} (1-\sigma)C_p^{\mathrm{T}} C_p & \mathbf{0} \\ \mathbf{0} & (1-\sigma)C_c^{\mathrm{T}} C_c \end{bmatrix} \\ Q_2 = \begin{bmatrix} -C_p^{\mathrm{T}} & \mathbf{0} \\ (1-\sigma)C_c^{\mathrm{T}} D_c & -C_c^{\mathrm{T}} \end{bmatrix} \\ Q_4 = \begin{bmatrix} I + (1-\sigma)D_c^{\mathrm{T}} D_c & -D_c^{\mathrm{T}} \\ -D_c & I \end{bmatrix} \end{cases}$$

where $\mathbf{0}$ is a zero matrix with proper dimension, and I is an identity matrix with appropriate dimension. It is obvious that $\mathcal{T}_e \subseteq \mathcal{T}_s$. According to [13, Th. V.2], if the hypotheses therein are satisfied, then the following hold for system (3)–(8).

1) It is globally exponential stable, i.e., $\exists c > 0$ and $\rho > 0$ s.t. $\forall \xi(0) \in \mathbb{R}^{n_\xi}$ with $w = 0$, $\|\xi(t)\| \leq ce^{-\rho t}\|\xi(0)\|$ for all $t \in \mathbb{R}^+$.
2) It has an $\mathcal{L}_2$-gain from w to z smaller than or equal to γ, i.e., $\exists \sigma : \mathbb{R}^{n_\xi} \to \mathbb{R}^+$ s.t. $\forall w \in \mathcal{L}_2, \xi(0) \in \mathbb{R}^{n_\xi}$, the corresponding solution to the system $z(t) := g(\xi(t), w(t))$ satisfies $\|z\|_{\mathcal{L}_2} \leq \sigma(\xi(0)) + \gamma\|w\|_{\mathcal{L}_2}$.

To model the timing behavior of a PETC system, we aim at constructing a power quotient system for this implementation.

Remark 3.1: Because of the uncertainty caused by the perturbation, it may happen that the perturbation compensates the effect of sampling, helping the state of the implementation to converge. Therefore, the event condition in (8) may not be satisfied along the timeline. As a result, there may not be an upper bound for the event intervals. However, an upper bound is necessary for constructing a useful power quotient system.

Remark 3.2: To apply scheduling approaches, an online scheduler is required. The model we are to construct is nondeterministic, i.e., after an event, the system may end up in several possible regions, but those regions are defined in terms of ξ_p, which means that from a measurement, it is not always clear in which region the system is. Thus, from simple output measurements, the online scheduler cannot figure out where the system is. Therefore, the online scheduler should be able to access the region in which the system is.

Assumption 3.3: The current state region at each event-triggered time t_b can be obtained in real time.

Because of the observation in Remark 3.1, we use the following event condition instead:

$$t_{b+1} = \inf \Big\{ t_k | t_k \in \mathcal{T}_s, t_k > t_b \\ \xi^{\mathrm{T}}(t_k) Q \xi(t_k) > 0 \bigvee t_k \geq t_b + \bar{\tau}_{\mathcal{R}(\xi(t_b))} \Big\} \tag{9}$$

where $\mathcal{R}(\xi(t_b))$ is the state region in state-space $\mathbb{R}^{n_\xi}$ at the last sampling time t_b, and $\bar{\tau}_{\mathcal{R}(\xi(t_b))}$ is a regional maximum allowable event interval (MAEI), which is dependent on $\mathcal{R}(\xi(t_b))$. According to Assumption 3.3, $\mathcal{R}(\xi(t_b))$ is obtainable. If this value cannot be accessed by the triggering mechanisms, one can always employ a global upper bound $\bar{\tau} :\geq \bar{\tau}_{\mathcal{R}(\xi(t_b))}$. We will discuss the computation of $\bar{\tau}_{\mathcal{R}(t_b)}$ in later sections. Note that, if the PETC implementation employing (8) can guarantee some predesigned stability and performance, then the PETC implementation employing (9) can guarantee the same stability and performance.

Consider the following period:

$$\tau(x) := t_{b+1} - t_b. \tag{10}$$

By definition $\hat{u}(t)$ is constant $\forall t \in [t_b, t_{b+1}[$ and dependent on $\xi_p(t_b)$ and $\xi_c(t_b)$. The input $\hat{u}(t)$ can be expressed as $\hat{u}(t) = C_E x$, $C_E := \begin{bmatrix} C_p & \mathbf{0} \\ D_c C_p & C_c \end{bmatrix}$, where $x := \begin{bmatrix} \xi_p^{\mathrm{T}}(t_b) & \xi_c^{\mathrm{T}}(t_b) \end{bmatrix}^{\mathrm{T}}$. Let $\xi_x(k) := \begin{bmatrix} \xi_p^{\mathrm{T}}(t_b + kh) & \xi_c^{\mathrm{T}}(t_b + kh) \end{bmatrix}^{\mathrm{T}}$ be the state evolution with initial state $x = \begin{bmatrix} \xi_p^{\mathrm{T}}(t_b) & \xi_c^{\mathrm{T}}(t_b) \end{bmatrix}^{\mathrm{T}}$, and $k \in \mathbb{N}$. Now, $\xi_x(k)$ can be computed as follows:

$$\xi_x(k) = M(k)x + \Theta(k) \tag{11}$$

where

$$M(k) := \begin{bmatrix} M_1(k) \\ M_2(k) \end{bmatrix}, \Theta(k) := \begin{bmatrix} \Theta_1(k) \\ \mathbf{0} \end{bmatrix}$$

$$\begin{cases} M_1(k) := \begin{bmatrix} I & \mathbf{0} \end{bmatrix} + \int_0^{kh} e^{A_p s} ds (A_p \begin{bmatrix} I & \mathbf{0} \end{bmatrix} \\ \qquad\qquad + B_p \begin{bmatrix} D_c C_p & C_c \end{bmatrix}) \\ M_2(k) := A_c^k \begin{bmatrix} \mathbf{0} & I \end{bmatrix} + \sum_{i=0}^{k-1} A_c^{k-1-i} B_c \begin{bmatrix} C_p & \mathbf{0} \end{bmatrix} \\ \Theta_1(k) := \int_0^{kh} e^{A_p (kh-s)} E w(s) ds. \end{cases}$$

Define $k(x) := \frac{\tau(x)}{h}$. From the event condition in (9), $k(x)$ can be computed as follows:

$$k(x) = \min\{\underline{k}(x), \overline{k}(x)\} \tag{12}$$

where $\overline{k}(x) := \frac{\bar{\tau}_{\mathcal{R}(x)}}{h}$ and

$$\underline{k}(x) := \inf \left\{ k \in \mathbb{N}^+ \middle| \begin{bmatrix} M(k)x + \Theta(k) \\ C_E x \end{bmatrix}^{\mathrm{T}} Q \begin{bmatrix} M(k)x + \Theta(k) \\ C_E x \end{bmatrix} > 0 \right\}. \tag{13}$$

Now, we present the main problem to be solved in this note. Consider the following system:

$$\mathcal{S} = (X, X_0, U, \longrightarrow, Y, H) \tag{14}$$

1) $X = \mathbb{R}^{n_x}$, $n_x = n_p + n_c$;
2) $X_0 \subseteq \mathbb{R}^{n_x}$;
3) $U = \emptyset$;
4) $\longrightarrow \subseteq X \times U \times X$ such that $\forall x, x' \in X : (x, x') \in \longrightarrow$ iff $\xi_x(H(x)) = x'$;
5) $Y \subset \mathbb{N}^+$;
6) $H : \mathbb{R}^{n_x} \to \mathbb{N}^+$, where $H(x) = k(x)$.

$\mathcal{S}$ is an infinite-state system. The output set Y of system $\mathcal{S}$ contains all the possible amount of sampling steps $\frac{t_{b+1} - t_b}{h} \in \mathbb{N}$, $b \in \mathbb{N}$ that the systems (3)–(7) and (9) may exhibit. Once the sampling time h is chosen, the event interval can then be computed by $k(x)h$.

Problem 3.4: Construct a finite abstraction of system $\mathcal{S}$ capturing enough information for scheduling.

Inspired by the work presented in [16], we solve this problem by constructing a power quotient system $\mathcal{S}_{/P}$ based on an adequately designed equivalence relation P defined over the state set X of $\mathcal{S}$. The constructed systems $\mathcal{S}_{/P}$ are semantically equivalent to timed automata, which can be used for automatic scheduler design [15].

In particular, the system $\mathcal{S}_{/P}$ to be constructed is as follows:

$$\mathcal{S}_{/P} = (X_{/P}, X_{/P,0}, U_{/P}, \underset{/P}{\longrightarrow}, Y_{/P}, H_{/P}) \tag{15}$$

1) $X_{/P} = \mathbb{R}^{n_x}_{/P} := \{\mathcal{R}_1, \ldots, \mathcal{R}_q\}$;
2) $X_{/P,0} = \mathbb{R}^{n_x}_{/P}$;
3) $(x_{/P}, x'_{/P}) \in \underset{/P}{\longrightarrow}$ if $\exists x \in x_{/P}$, $\exists x' \in x'_{/P}$ such that $\xi_x(H(x)) = x'$;
4) $Y_{/P} \subset 2^Y \subset \mathbb{IN}^+$;
5) $H_{/P}(x_{/P}) = [\min_{x\in x_{/P}} H(x), \max_{x\in x_{/P}} H(x)] := [\underline{k}(x_{/P}), \bar{k}(x_{/P})]$.

$\mathcal{S}_{/P}$ is a finite state system. Compared with the power quotient system constructed in [16], a main difference is that since we focus on PETC, there is no timing uncertainty.

IV. Construction of the Quotient System

A. State Set

From the results presented in [8], we remark the following fact.

Remark 4.1: When $w = 0$, excluding the origin, all the states that lie on a line going through the origin have an identical triggering behavior.

We also call the following assumption.

Assumption 4.2: The perturbation w satisfies $w \in \mathcal{L}_2$ and $w \in \mathcal{L}_\infty$. Besides, assume that an upper bound $\mathcal{W} > 0$ for $\|w\|_{\mathcal{L}_\infty}$, i.e., $\|w\|_{\mathcal{L}_\infty} \leq \mathcal{W}$, is known.

Based on Remark 4.1 and Assumption 4.2, we propose the state-space partition as follows:

$$\mathcal{R}_{s_1,s_2} = \left\{ x \in \mathbb{R}^{n_x} \left| \bigwedge_{i=1}^{n_x-1} x^{\mathrm{T}} \Xi_{s_1,(i,i+1)} x \geq 0 \bigwedge W_{s_2-1} \leq |x| < W_{s_2} \right. \right\} \tag{16}$$

where $s_1 \in \{1, \ldots, q_1\}$, $s_2 \in \{1, \ldots, q_2\}$, and $q_1, q_2 \in \mathbb{N}$ are pre-designed scalars. $\Xi_{s_1,(i,j)}$ is a constructed matrix, and $\{W_i | i \in \{0, \ldots, q_2\}\}$ is a sequence of scalars. Note that $W_0 = 0$, $W_{q_2} = +\infty$, and the remaining W_{s_2} are bounded and somewhere in between 0 and $+\infty$. It is obvious that $\bigcup_{s_1\in\{1,\ldots,q_1\}, s_2\in\{1,\ldots,q_2\}} \mathcal{R}_{s_1,s_2} = \mathbb{R}^{n_x}$.

This state-space partition combines partitioning the state-space into a finite number of polyhedral cones (named *isotropic covering* [8]) and finite homocentric spheres. From (16), we can see that the *isotropic covering* describes the relation between entries of the state vector, while the *transverse isotropic covering* is used to capture the relation between the norm of the state vector and the $\mathcal{L}_\infty$ norm of the perturbations, which will be shown later in Theorem 4.4. If $w = 0$, the homocentric spheres can be omitted. Details on the *isotropic covering* can be found in the Appendix. Fig. 1 shows a two-dimensional (2-D) example.

B. Output Map

We, first, free the system dynamics from the uncertainty caused by the perturbation.

Lemma 4.3: Consider the systems (3)–(7) and (9) and that Assumption 4.2 holds. If there exist a scalar $\mu \geq 0$ and a symmetric matrix Ψ such that $(Q_1 + \Psi)_1 \preceq \mu I$, then $\underline{k}(x)$ generated by (13) is lower bounded by

$$k'(x) := \inf\{k \in \mathbb{N}^+ | \Phi(k) \succ 0\} \tag{17}$$

where

$$Q_1 + \Psi = \begin{bmatrix} (Q_1+\Psi)_1 & (Q_1+\Psi)_2 \\ (Q_1+\Psi)_3 & (Q_1+\Psi)_4 \end{bmatrix}$$

$$(Q_1+\Psi)_1 \in \mathbb{R}^{n_p \times n_p}$$

$$\Phi(k) := \begin{bmatrix} \Phi_1(k) & \Phi_2(k) & \mathbf{0} \\ \Phi_2^{\mathrm{T}}(k) & -\Psi & \mathbf{0} \\ \mathbf{0} & \mathbf{0} & \Phi_3(k) \end{bmatrix} \tag{18}$$

$$\begin{cases} \Phi_1(k) = M^{\mathrm{T}}(k) Q_1 M(k) + M^{\mathrm{T}}(k) Q_2 C_E \\ \qquad\qquad + C_E^{\mathrm{T}} Q_2^{\mathrm{T}} M(k) + C_E^{\mathrm{T}} Q_4 C_E \\ \Phi_2(k) = M^{\mathrm{T}}(k) Q_1 + C_E^{\mathrm{T}} Q_2^{\mathrm{T}} \\ \Phi_3(k) = kh\mu\lambda_{\max}(E^{\mathrm{T}}E) d_{A_p}(k) \end{cases} \tag{19}$$

$$d_{A_p}(k) = \begin{cases} \dfrac{e^{k\lambda_{\max}(A_p + A_p^{\mathrm{T}})} - 1}{\lambda_{\max}(A_p + A_p^{\mathrm{T}})}, & \text{if } \lambda_{\max}(A_p + A_p^{\mathrm{T}}) \neq 0 \\ kh, & \text{if } \lambda_{\max}(A_p + A_p^{\mathrm{T}}) = 0 \end{cases}.$$

Next, we construct LMIs that bridge Lemma 4.3 and the state-space partition.

Theorem 4.4: (Regional lower bound): Consider a scalar $\underline{k}_{s_1,s_2} \in \mathbb{N}$ and regions with $s_2 > 1$. If the hypothesis in Lemma 4.3 holds and there exist scalars $\varepsilon_{k,(s_1,s_2),(i,i+1)} \geq 0$, where $i \in \{1, \ldots, n_x - 1\}$, such that for all $k \in \{0, \ldots, \underline{k}_{s_1,s_2}\}$, the following LMIs hold:

$$\begin{bmatrix} H & \Phi_2(k) \\ \Phi_2^{\mathrm{T}}(k) & -\Psi \end{bmatrix} \preceq 0 \tag{20}$$

where $H = \Phi_1(k) + \Phi_3(k)\mathcal{W}^2 W_{s_2-1}^{-2} I + \sum_{i\in\{1,\ldots,n_x-1\}} \varepsilon_{k,(s_1,s_2),(i,i+1)} \Xi_{s_1,(i,i+1)}$, with $\Phi_1(k)$, $\Phi_2(k)$, and $\Phi_3(k)$ defined in (19), and Ψ from Lemma 4.3, then the interevent times (9) for systems (3)–(7) are regionally bounded from below by $(\underline{k}_{s_1,s_2} + 1)h$. For the regions with $s_2 = 1$, the regional lower bound is h.

Remark 4.5: In Theorem 4.4, we discuss the situations when $s_2 > 1$ and $s_2 = 1$ since for all regions with $s_2 > 1$, $W_{s_2-1} \neq 0$ holds, while for all regions with $s_2 = 1$, $W_{s_2-1} = 0$ holds. When $W_{s_2-1} \neq 0$, one can easily validate the feasibility of the LMI (20), whereas when $W_{s_2-1} = 0$, H will be diagonal infinity, making the LMI (20) infeasible when $k > 0$. However, according to the property of PETC, i.e., $t_{b+1} \in \mathcal{T}_s$ and $t_{b+1} > t_b$, the regional lower bound exists and is equal to h.

Remark 4.6: Consider the systems (3)–(7), (9), and (16). In order to find all the regional lower bounds by the approach presented in Theorem 4.4, a maximum of $\sum_{s_1\in\{1,\ldots,q_1\}, s_2\in\{1,\ldots,q_2\}} (\underline{k}_{s_1,s_2} \times q_1 \times q_2)$ LMIs

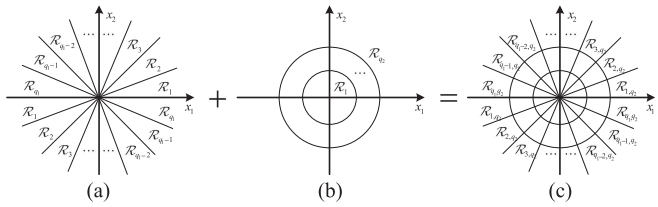

Fig. 1. Example of the state-space partition into (a) finite number of polyhedral cones, (b) finite number of homocentric spheres, and (c) finite number of regions.

are required to be solved. Each LMI has $(n_x - 1)$ decision variables, and the dimension of the matrix in each LMI is $2n_x \times 2n_x$.

Following similar ideas as in Theorem 4.4, we present, next, lower and upper bounds starting from each state partition when $w = 0$. Consider the following event condition:

$$k(x) = \inf \left\{ k \in \mathbb{N}^+ | \begin{bmatrix} M(k)x \\ C_E x \end{bmatrix}^{\mathrm{T}} Q \begin{bmatrix} M(k)x \\ C_E x \end{bmatrix} > 0 \right\}. \tag{21}$$

Remark 4.7: Since (21) does not consider perturbations when computing the lower and upper bounds for each region, according to Remark 4.1, applying the *isotropic covering* is enough.

We define $\mathcal{R}_{s_1,\bullet}$ to represent $\mathcal{R}_{s_1,s_2}\ \forall s_2 \in \{1,\dots,q_2\}$.

Corollary 4.8: (Regional lower bound when $w = 0$): Consider a scalar $\underline{k}_{s_1,\bullet} \in \mathbb{N}$. If there exist scalars $\underline{\varepsilon}_{k,s_1,(i,i+1)} \geq 0$, where $i \in \{1,\dots,n_x - 1\}$, such that for all $k \in \{0,\dots,\underline{k}_{s_1,\bullet}\}$, the following LMIs hold:

$$\Phi_1(k) + \sum_{i\in\{1,\dots,n_x-1\}} \underline{\varepsilon}_{k,s_1,(i,i+1)} \Xi_{s_1,(i,i+1)} \preceq 0 \tag{22}$$

with $\Phi_1(k)$ defined in (19), then the interevent times (8) of the systems (3)–(7) with $w = 0$ are regionally bounded from below by $(\underline{k}_{s_1,\bullet} + 1)h$.

Corollary 4.9: (Regional upper bound when $w = 0$): Let $\bar{l} \in \mathbb{N}$ be a large enough scalar. Consider a scalar $\bar{k}_{s_1,\bullet} \in \{\underline{k}_{s_1,\bullet},\dots,\bar{l}\}$. If there exist scalars $\bar{\varepsilon}_{k,s_1,(i,i+1)} \geq 0$, where $i \in \{1,\dots,n_x - 1\}$, such that for all $k \in \{\bar{k}_{s_1,\bullet},\dots,\bar{l}\}$, the following LMIs hold:

$$\Phi_1(k) - \sum_{i\in\{1,\dots,n_x-1\}} \bar{\varepsilon}_{k,s_1,(i,i+1)} \Xi_{s_1,(i,i+1)} \succ 0 \tag{23}$$

with $\Phi_1(k)$ defined in (19), then the interevent times (8) of the systems (3)–(7) with $w = 0$ are regionally bounded from above by $\bar{k}_{s_1,\bullet}h$.

Remark 4.10: For the choice of $\bar{l}$, we follow [16, Rem. 2] and apply a line search approach: Increasing $\bar{l}$ until $\Phi_1(\bar{l}) \succ 0$. This results in $\bar{l}$ being a global upper bound for the interevent time (8) of the systems (3)–(7) with $w = 0$.

It is obvious that $\bar{l} \geq \bar{k}_{s_1,\bullet} > \underline{k}_{s_1,\bullet} \geq \underline{k}_{s_1,s_2}\ \forall s_2$. We can, now, set the regional MAEI $\bar{\tau}_{\mathcal{R}(\xi(t_b))}$ in (9) as $\bar{\tau}_{\mathcal{R}(\xi(t_b))} := \bar{k}_{s_1,\bullet}h\ \forall x \in \mathcal{R}_{s_1,\bullet}$.

C. Transition Relation

In this section, we discuss the construction of the transition relation and the reachable state set. Denote the initial state set as $X_{0,(s_1,s_2)}$, after kth samplings without an update, and the reachable state set is denoted as $X_{k,(s_1,s_2)}$. According to (11), a relation can be obtained as follows:

$$X_{k,(s_1,s_2)} = M(k)X_{0,(s_1,s_2)} + \Theta(k). \tag{24}$$

It is obvious that $X_{k,(s_1,s_2)}$ cannot be computed directly because the perturbation is uncertain and the state region may not be convex. Therefore, we aim to find sets $\hat{X}_{k,(s_1,s_2)}$ such that $X_{k,(s_1,s_2)} \subseteq \hat{X}_{k,(s_1,s_2)}$. To compute $\hat{X}_{k,(s_1,s_2)}$, we take the following steps.

1) Partition the Dynamics: According to (24), $\hat{X}_{k,(s_1,s_2)}$ can be computed by $\hat{X}_{k,(s_1,s_2)} = \hat{X}^1_{k,(s_1,s_2)} \oplus \hat{X}^2_{k,(s_1,s_2)}$, where $\oplus$ is the Minkowski addition, and $\hat{X}^1_{k,(s_1,s_2)}$ and $\hat{X}^2_{k,(s_1,s_2)}$ are sets to be computed.

2) Compute $\hat{X}^1_{k,(s_1,s_2)}$: One can compute $\hat{X}^1_{k,(s_1,s_2)}$ by $\hat{X}^1_{k,(s_1,s_2)} = M(k)\hat{X}_{0,(s_1,s_2)}$, where $\hat{X}_{0,(s_1,s_2)}$ is a polytope that overapproximates $X_{0,(s_1,s_2)}$, i.e., $X_{0,(s_1,s_2)} \subseteq \hat{X}_{0,(s_1,s_2)}$. $\hat{X}_{0,(s_1,s_2)}$ can be computed as in the optimization problem [2, eq. (1)].

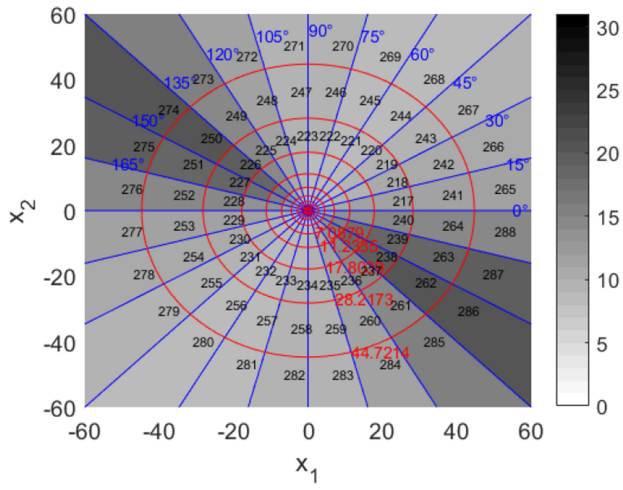

Fig. 2. Computed result of the regional lower bound with $\mathcal{W} = 2$.

3) Compute $\hat{X}^2_{k,(s_1,s_2)}$: For the computation of $\hat{X}^2_{k,(s_1,s_2)}$, it follows that $\hat{X}^2_{k,(s_1,s_2)} = \{x \in \mathbb{R}^{n_x} | |x| \leq |\Theta(k)|\}$, where $|\Theta(k)| = |\int_0^{kh} e^{A_p(kh-s)}Ew(s)ds| \leq \int_0^{kh} |e^{A_p(kh-s)}Ew(s)|ds \leq \int_0^{kh} |e^{A_p(kh-s)}||ds|E||w\|_{\mathcal{L}_\infty} \leq \int_0^{kh} e^{\lambda_{\max}(\frac{A_p^{\mathrm{T}}+A_p}{2})(kh-s)}ds|E|\mathcal{W}$, in which the last inequation holds according to [25, eq. (2.2)].

Thus, the reachable set $X_{\{\underline{k}_{s_1,s_2},\bar{k}_{s_1,\bullet}\},(s_1,s_2)}$ of the systems (3)–(7) and (9), starting from $X_{0,(s_1,s_2)}$, can be computed by $X_{\{\underline{k}_{s_1,s_2},\bar{k}_{s_1,\bullet}\},(s_1,s_2)} \subseteq \hat{X}_{\{\underline{k}_{s_1,s_2},\bar{k}_{s_1,\bullet}\},(s_1,s_2)} = \bigcup_{k\in\{\underline{k}_{s_1,s_2},\dots,\bar{k}_{s_1,\bullet}\}} \hat{X}_{k,(s_1,s_2)}$.

To compute the transitions in $\mathcal{S}_{/P}$, one can check the intersection between the overapproximation of the reachable state set and all the state regions $\mathcal{R}_{s_1',s_2'}\ \forall s_1' \in \{1,\dots,q_1\}, s_2' \in \{1,\dots,q_2\}$. More specifically, one can check if the following feasibility problem for each state region holds $\mathcal{R}_{s_1',s_2'} \cap \hat{X}_{\{\underline{k}_{s_1,s_2},\bar{k}_{s_1,\bullet}\},(s_1,s_2)} \neq \emptyset$, in which case $(\mathcal{R}_{s_1,s_2}, \mathcal{R}_{s_1',s_2'}) \in \underset{/P}{\longrightarrow}$.

D. Main Result

Now, we summarize the main result of this note in the following theorem.

Theorem 4.11: The metric system $\mathcal{S}_{/P} = (X_{/P}, X_{/P,0}, U_{/P}, \underset{/P}{\longrightarrow}, Y_{/P}, H_{/P})$ ϵ-approximately simulates $\mathcal{S}$, where $\epsilon = \max d_H(y,y')$, $y = H(x) \in Y$, $y' = H_{/P}(x') \in Y_{/P}\ \forall (x,x') \in P$, and $d_H(\cdot,\cdot)$ is the Hausdorff distance.

V. Numerical Example

In this section, we consider a system employed in [13] and [23]. The plant is given by $\dot{\xi}(t) = \begin{bmatrix} 0 & 1 \\ -2 & 3 \end{bmatrix}\xi(t) + \begin{bmatrix} 0 \\ 1 \end{bmatrix}v(t) + \begin{bmatrix} 1 \\ 0 \end{bmatrix}w(t)$, and the control gain is given by $K = \begin{bmatrix} 1 & -4 \end{bmatrix}$. This plant is chosen since it is easy to show the feasibility of the presented theory in 2-D plots. Letting $q_1 = 24$ and $q_2 = 12$, the state-space is divided into 288 regions. The state-space partition is shown in Fig. 2, where regions are labeled by natural numbers counterclockwise and from inner regions to outer ones, starting from the positive horizontal axis. We set $\mathcal{W} = 2$, the convergence rate $\rho = 0.01$, $\mathcal{L}_2$ gain $\gamma = 2$, sampling time $h = 0.005$ s, and event condition $\sigma = 0.1$. By checking the LMI presented in [13], we can see that there exists a feasible solution; thus, the

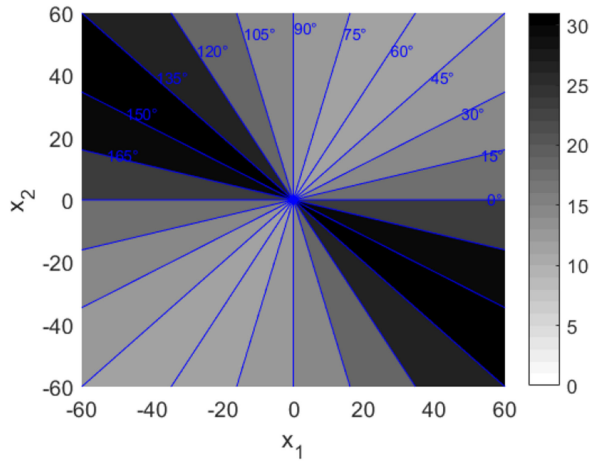

Fig. 3. Computed result of the regional upper bound with $w = 0$.

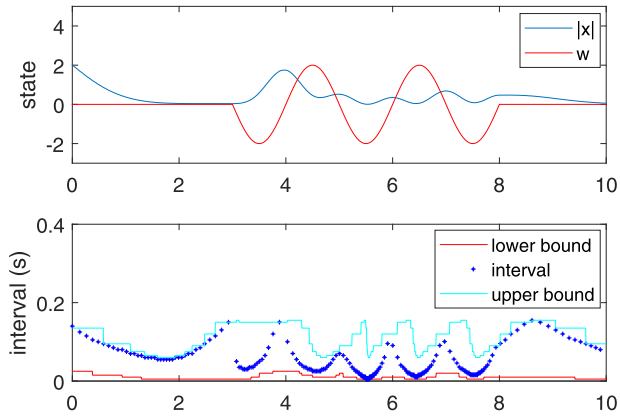

Fig. 4. System evolution and event intervals when $w = 2\sin(\pi t), t \in [3, 8]$: State evaluation and perturbance, event intervals with the bounds.

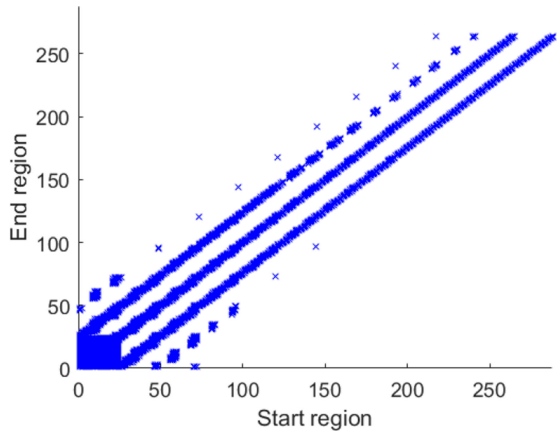

Fig. 5. Reachable regions, starting from each state region, with labeling from Fig. 2.

stability and performance can be guaranteed. The result of the computed lower bound by Theorem 4.4 is shown in Fig. 2. The computed upper bound by Corollary 4.9 is shown in Fig. 3. The resulting abstraction precision is $\epsilon = 0.15$ s. The simulation results of the system evolution and event intervals with perturbations are shown in Fig. 4. The upper bound triggered six events during the 10-s simulation. Note that increasing the number of subdivisions can lead to less conserved

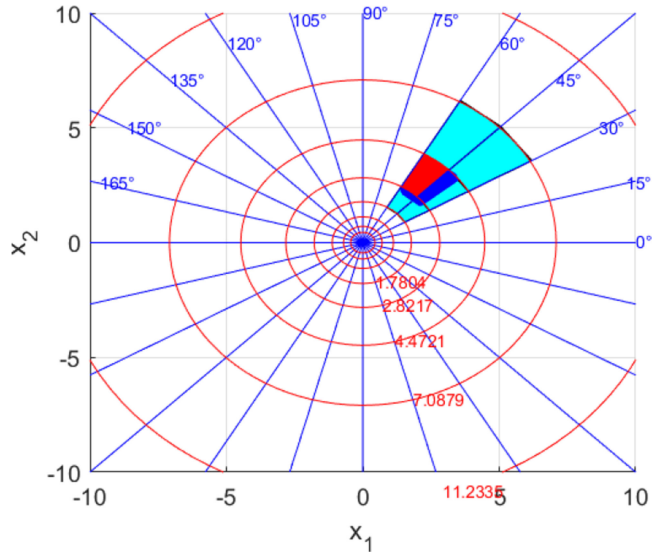

Fig. 6. Flow pipe of $(s_1, s_2) = (4, 6)$ indicating the initial state set (red), the reachable state set (blue), and reachable regions (cyan).

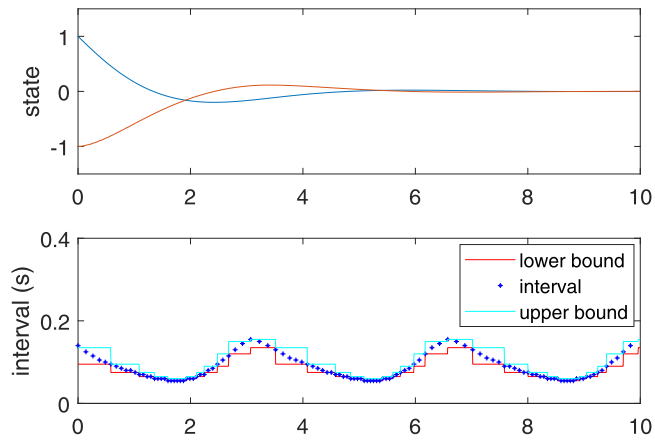

Fig. 7. System evolution and event intervals when $w = 0$: State evaluation and event intervals versus computed bounds.

lower and upper bounds of the interevent time. The conservativeness can also be reduced by decreasing $\mathcal{W}$. The reachable state regions, starting from each region, are shown in Fig. 5. As an example, the reachable state region of the initial region $(s_1, s_2) = (4, 6)$ is shown in Fig. 6. We also present a simulation when $w = 0$. The evolution of the system is shown in Fig. 7, which shows that the interevent intervals are within the computed bounds.

VI. Conclusion

In this note, we present the construction of a power quotient system for the traffic model of the PETC implementations from [13]. The constructed models can be used to estimate the next event time and the state set when the next event occurs. These models allow to design scheduling to improve the listening time of wireless communications and the medium access time to increase the energy consumption and bandwidth occupation efficiency. In this note, we consider an output feedback system with a dynamic controller. However, the state partition is still based on the states of the system and controller. The system state may not always be obtainable. Therefore, to estimate the system state in an ETC implementation from output measurements is a very important

extension to make this note more practical. The periodic asynchronous event-triggered control presented in [10] is an extension of the PETC considering quantization. Since the dynamics of the quantization error are dependent on the states, one can either treat the quantization error as part of the perturbations or analyze this part separately to increase the abstraction precision. This is also an interesting future investigation. Another interesting extension is the reconstruction of traffic models for each sensor node to capture the local timing behavior in a decentralized PETC implementation by using either global information or even only local information.

APPENDIX

Isotropic Covering: Consider $x = \begin{bmatrix} x_1 & x_2 & \cdots & x_n \end{bmatrix}^{\mathrm{T}} \in \mathbb{R}^n$. We, first, present a case when $x \in \mathbb{R}^2$. Let $\Theta = [-\frac{\pi}{2}, \frac{\pi}{2}[$ be an interval. Split this interval into q subintervals, and let $\Theta_s = [\underline{\theta}_s, \overline{\theta}_s[$ be the sth subinterval. Then, for each subinterval, one can construct a cone pointing at the origin: $\mathcal{R}_s = \{x \in \mathbb{R}^2 | x^{\mathrm{T}} \tilde{\Xi}_s x \geq 0\}$, where $\tilde{\Xi}_s = \begin{bmatrix} -\sin\underline{\theta}_s \sin\overline{\theta}_s & \frac{1}{2}\sin(\underline{\theta}_s + \overline{\theta}_s) \\ \frac{1}{2}\sin(\underline{\theta}_s + \overline{\theta}_s) & -\cos\underline{\theta}_s \cos\overline{\theta}_s \end{bmatrix}$. Remark 4.1 shows that x and $-x$ have the same behavior; therefore, it is sufficient to only consider half of the state space.

Now, we derive the case when $x \in \mathbb{R}^n$, $n > 2$. Define $(x)_{i,j} = (x_i, x_j)$ as the projection of this point on its i–j coordinate plane. Now, a polyhedral cone $\mathcal{R}_s$ can be defined as $\mathcal{R}_s = \{x \in \mathbb{R}^n | \bigwedge_{i=1}^{n-1} (x)_{(i,i+1)}^{\mathrm{T}} \tilde{\Xi}_{s,(i,i+1)} (x)_{(i,i+1)} \geq 0\}$, where $\tilde{\Xi}_{s,(i,i+1)}$ is a constructed matrix. A relation between $\tilde{\Xi}_{s,(i,i+1)}$ and $\Xi_{s,(i,i+1)}$ from (16) is given by $[\Xi_{s,(i,i+1)}]_{(i,i)} = [\tilde{\Xi}_{s,(i,i+1)}]_{(1,1)}$, $[\Xi_{s,(i,i+1)}]_{(i,i+1)} = [\tilde{\Xi}_{s,(i,i+1)}]_{(1,2)}$, $[\Xi_{s,(i,i+1)}]_{(i+1,i)} = [\tilde{\Xi}_{s,(i,i+1)}]_{(2,1)}$, $[\Xi_{s,(i,i+1)}]_{(i+1,i+1)} = [\tilde{\Xi}_{s,(i,i+1)}]_{(2,2)}$, and $[\Xi_{s,(i,i+1)}]_{(k,l)} = 0$, where $[M]_{(i,j)}$ is the ith row jth column entry of the matrix M, and k and l satisfy $(k,l) \neq (i, i+1)$. ■

Proof of Lemma 4.3: First, we decouple the event-triggering mechanism in (13) as follows:

$$\begin{aligned} &\begin{bmatrix} M(k)x + \Theta(k) \\ C_E x \end{bmatrix}^{\mathrm{T}} Q \begin{bmatrix} M(k)x + \Theta(k) \\ C_E x \end{bmatrix} \\ &\quad = x^{\mathrm{T}}\Phi_1(k)x + x^{\mathrm{T}}\Phi_2(k)\Theta(k) + \Theta^{\mathrm{T}}(k)\Phi_2^{\mathrm{T}}(k)x \\ &\qquad + \Theta^{\mathrm{T}}(k)Q_1\Theta(k) \\ &\quad \leq x^{\mathrm{T}}(\Phi_1(k) + \Phi_2(k)\Psi^{-1}\Phi_2^{\mathrm{T}}(k))x + \Theta^{\mathrm{T}}(k)(Q_1 + \Psi)\Theta(k) \end{aligned} \tag{25}$$

where the last inequality comes from [12, Lem. 6.2]. Now, for the uncertainty part, we have $\Theta^{\mathrm{T}}(k)(Q_1 + \Psi)\Theta(k) = \begin{bmatrix} \Theta_1(k) \\ \mathbf{0} \end{bmatrix}^{\mathrm{T}} \begin{bmatrix} (Q_1+\Psi)_1 & (Q_1+\Psi)_2 \\ (Q_1+\Psi)_3 & (Q_1+\Psi)_4 \end{bmatrix} \begin{bmatrix} \Theta_1(k) \\ \mathbf{0} \end{bmatrix} = \Theta_1^{\mathrm{T}}(k)(Q_1 + \Psi)_1\Theta_1(k)$. From the hypothesis of the theorem that there exists μ such that $(Q_1 + \Psi)_1 \preceq \mu I$, together with Jensen's inequality [12], inequality [25, eq. (2.2)], and Assumption 4.2, i.e., $w \in \mathcal{L}_\infty$, $\Theta^{\mathrm{T}}(k)(Q_1 + \Psi)\Theta(k)$ can be bounded from above by (see [9, Proof of Th. 2])

$$\Theta^{\mathrm{T}}(k)(Q_1 + \Psi)\Theta(k) \leq kh\mu\lambda_{\max}(E^{\mathrm{T}}E)d_{A_p}(k)\|w\|_{\mathcal{L}_\infty}^2. \tag{26}$$

With (26), (25) can be further bounded as follows:

$$\begin{aligned} &\begin{bmatrix} M(k)x + \Theta(k) \\ C_E x \end{bmatrix}^{\mathrm{T}} Q \begin{bmatrix} M(k)x + \Theta(k) \\ C_E x \end{bmatrix} \\ &\quad \leq x^{\mathrm{T}}(\Phi_1(k) + \Phi_2(k)\Psi^{-1}\Phi_2^{\mathrm{T}}(k))x + \Phi_3(k)\|w\|_{\mathcal{L}_\infty}^2. \end{aligned} \tag{27}$$

From the hypothesis of the theorem, if $\Phi(k) \preceq 0$ holds, then by applying the Schur complement to (18), the following inequality holds $x^{\mathrm{T}}(\Phi_1(k) + \Phi_2(k)\Psi^{-1}\Phi_2^{\mathrm{T}}(k))x + \Phi_3(k)\|w\|_{\mathcal{L}_\infty}^2 \leq 0$, which indicates

$$\begin{bmatrix} M(k)x + \Theta(k) \\ C_E x \end{bmatrix}^{\mathrm{T}} Q \begin{bmatrix} M(k)x + \Theta(k) \\ C_E x \end{bmatrix} \leq 0. \tag{28}$$

Therefore, $\underline{k}(x)$ generated by (13) is lower bounded by $k'(x)$ generated by (17). This ends the proof. ■

Proof of Theorem 4.4: We, first, consider the regions with $s_2 > 1$. If all the hypotheses of the theorem hold, then by applying the Schur complement to (20), one has

$$x^{\mathrm{T}}(H + \Phi_2(k)\Psi^{-1}\Phi_2^{\mathrm{T}}(k))x \leq 0. \tag{29}$$

From (16), and applying the S-procedure, the following holds:

$$x^{\mathrm{T}}(\Phi_1(k) + \Phi_3(k)\mathcal{W}^2 W_{s_2-1}^{-2} I + \Phi_2(k)\Psi^{-1}\Phi_2^{\mathrm{T}}(k))x \leq 0. \tag{30}$$

From (16), we also have $x^{\mathrm{T}}x \geq W_{s_2-1}^2$. Since $\Phi_3(k)$, $\mathcal{W}$, and W_{s_2-1} are nonnegative scalars and $W_{s_2-1} > 0$, we have the following inequality:

$$\begin{aligned} x^{\mathrm{T}}\Phi_3(k)\mathcal{W}^2 W_{s_2-1}^{-2} Ix &= \Phi_3(k)\mathcal{W}^2 W_{s_2-1}^{-2} x^{\mathrm{T}}x \\ &\geq \Phi_3(k)\mathcal{W}^2 W_{s_2-1}^{-2} W_{s_2-1}^2 = \Phi_3(k)\mathcal{W}^2 \geq \Phi_3(k)\|w\|_{\mathcal{L}_\infty}^2 \end{aligned} \tag{31}$$

in which the last inequality comes form the definition of $\mathcal{W}$. Now, inserting (31) into (30) yields

$$x^{\mathrm{T}}(\Phi_1(k) + \Phi_2(k)\Psi^{-1}\Phi_2^{\mathrm{T}}(k))x + \Phi_3(k)\|w\|_{\mathcal{L}_\infty}^2 \leq 0$$

which together with applying the Schur complement to (18) provides the regional lower bound.

When $s_2 = 1$, $k > 0$, the diagonal elements of H will be infinity. Thus, one cannot find a feasible solution to the LMI (20). According to the event-triggered condition (9), which indicates that $t_{b+1} \in \mathcal{T}_s$ and $t_{b+1} > t_b$, the regional lower bound for those regions with $s_2 = 1$ is h. This finishes the proof. ■

Proof of Corollary 4.8: The result can be easily obtained from Theorem 4.4 by considering $E = \mathbf{0}$. ■

Proof of Corollary 4.9: The result can be easily obtained analogously to Theorem 4.4 by considering $E = \mathbf{0}$: If all the hypotheses of this corollary hold, then according to (23), $\Phi_1(k) \succ 0$, $k \in \{\bar{k}_{s_1,\bullet}, \ldots, \bar{l}\}$. According to the definition of $\Phi_1(k)$ in (19), for all $k \geq \bar{k}_{s_1,\bullet}$, $\begin{bmatrix} M(k)x \\ C_E x \end{bmatrix}^{\mathrm{T}} Q \begin{bmatrix} M(k)x \\ C_E x \end{bmatrix} > 0$ holds, which together with event condition (21) provides the regional upper bound. ■

Proof of Theorem 4.11: The result follows from Lemma 2.7 and the construction described in Section IV. ■

REFERENCES

[1] F. Cassez, A. David, E. Fleury, K. G. Larsen, and D. Lime, "Efficient on-the-fly algorithms for the analysis of timed games," in *CONCUR 2005—Concurrency Theory*, M. Abadi and L. de Alfaro, Eds., Berlin, Germany: Springer, 2005, pp. 66–80.

[2] A. Chutinan and B. H. Krogh, "Computational techniques for hybrid system verification," *IEEE Trans. Autom. Control*, vol. 48, no. 1, pp. 64–75, Jan. 2003.

[3] M. B. G. Cloosterman, L. Hetel, N. van de Wouw, W. P. M. H. Heemels, J. Daafouz, and H. Nijmeijer, "Controller synthesis for networked control systems," *Automatica*, vol. 46, no. 10, pp. 1584–1594, 2010.

[4] M. B. G. Cloosterman, N. van de Wouw, W. P. M. H. Heemels, and H. Nijmeijer, "Stability of networked control systems with uncertain time-varying delays," *IEEE Trans. Autom. Control*, vol. 54, no. 7, pp. 1575–1580, Jul. 2009.

[5] M. C. F. Donkers and W. P. M. H. Heemels, "Output-based event-triggered control with guaranteed-gain and improved and decentralized event-triggering," *IEEE Trans. Autom. Control*, vol. 57, no. 6, pp. 1362–1376, Jun. 2012.
[6] M. C. F. Donkers, W. P. M. H. Heemels, N. van de Wouw, and L. Hetel, "Stability analysis of networked control systems using a switched linear systems approach," *IEEE Trans. Autom. Control*, vol. 56, no. 9, pp. 2101–2115, Sep. 2011.
[7] G. Ewald, *Combinatorial Convexity and Algebraic Geometry*, vol. 168. New York, NY, USA: Springer-Verlag, 2012.
[8] C. Fiter, L. Hetel, W. Perruquetti, and J.-P. Richard, "A state dependent sampling for linear state feedback," *Automatica*, vol. 48, no. 8, pp. 1860–1867, 2012.
[9] C. Fiter, L. Hetel, W. Perruquetti, and J.-P. Richard, "A robust stability framework for LTI systems with time-varying sampling," *Automatica*, vol. 54, pp. 56–64, 2015.
[10] A. Fu and M. Mazo Jr, "Decentralized periodic event-triggered control with quantization and asynchronous communication," *Automatica*, vol. 94, pp. 294–299, 2018.
[11] R. H. Gielen, S. Olaru, M. Lazar, W. P. M. H. Heemels, N. van de Wouw, and S.-I. Niculescu, "On polytopic inclusions as a modeling framework for systems with time-varying delays," *Automatica*, vol. 46, no. 3, pp. 615–619, 2010.
[12] K. Gu, J. Chen, and V. L Kharitonov, *Stability of Time-Delay Systems*. New York, NY, USA: Springer-Verlag, 2003.
[13] W. P. M. H. Heemels, M. C. F. Donkers, and A. R. Teel, "Periodic event-triggered control for linear systems," *IEEE Trans. Autom. Control*, vol. 58, no. 4, pp. 847–861, Apr. 2013.
[14] L. Hetel, J. Daafouz, and C. Iung, "Stabilization of arbitrary switched linear systems with unknown time-varying delays," *IEEE Trans. Autom. Control*, vol. 51, no. 10, pp. 1668–1674, Oct. 2006.
[15] A. S. Kolarijani, D. Adzkiya, and M. Mazo, "Symbolic abstractions for the scheduling of event-triggered control systems," in *Proc. 54th IEEE Conf. Decis. Control*, 2015, pp. 6153–6158.
[16] A. S. Kolarijani and M. Mazo Jr, "A formal traffic characterization of LTI event-triggered control systems," *IEEE Trans. Control Netw. Syst.*, vol. 5, no. 1, pp. 274–283, Mar. 2018.
[17] A. S. Kolarijani, M. Mazo Jr, and T. Keviczky, "Timing abstraction of perturbed LTI systems with l2-based event-triggering mechanism," in *Proc. IEEE 55th Conf. Decis. Control*, 2016, pp. 1364–1369.
[18] M. Mazo Jr, and M. Cao, "Asynchronous decentralized event-triggered control," *Automatica*, vol. 50, no. 12, pp. 3197–3203, 2014.
[19] M. Mazo Jr. and A. Fu, "Decentralized event-triggered controller implementations," in *Event-Based Control and Signal Processing*, M. Miskowicz, Ed., Boca Raton, FL, USA: CRC Press, 2015, pp. 121–150, [Online]. Available: https://www.crcpress.com/Event-Based-Control-and-Signal-Processing/Miskowicz/p/book/9781138893184
[20] M. Mazo Jr, and P. Tabuada, "Decentralized event-triggered control over wireless sensor/actuator networks," *IEEE Trans. Autom. Control*, vol. 56, no. 10, pp. 2456–2461, Oct. 2011.
[21] J. Skaf and S. Boyd, "Analysis and synthesis of state-feedback controllers with timing jitter," *IEEE Trans. Autom. Control*, vol. 54, no. 3, pp. 652–657, Mar. 2009.
[22] Y. S. Suh, "Stability and stabilization of nonuniform sampling systems," *Automatica*, vol. 44, no. 12, pp. 3222–3226, 2008.
[23] P. Tabuada, "Event-triggered real-time scheduling of stabilizing control tasks," *IEEE Trans. Autom. Control*, vol. 52, no. 9, pp. 1680–1685, Sep. 2007.
[24] P. Tabuada, *Verification and Control of Hybrid Systems: A Symbolic Approach*. New York, NY, USA: Springer-Verlag, 2009.
[25] C. Van Loan, "The sensitivity of the matrix exponential," *SIAM J. Numer. Anal.*, vol. 14, no. 6, pp. 971–981, 1977.
[26] X. Wang and M. D. Lemmon, "Event-triggering in distributed networked control systems," *IEEE Trans. Autom. Control*, vol. 56, no. 3, pp. 586–601, Mar. 2011.
[27] X. Wang and M. D. Lemmon, "On event design in event-triggered feedback systems," *Automatica*, vol. 47, no. 10, pp. 2319–2322, 2011.